Weakly bound (6s1/2 + 6p1/2)0g Cs2 levels analysed using the vibrational quantum defect: detection of two deeply bound (6s1/2 + 6p3/2)0g levels

L Pruvost, H Jelassi

Weakly bound $(6s_{1/2}+6p_{1/2})0_g^-$ Cs_2 levels analysed using the vibrational quantum defect. Detection of two deeply bound $(6s_{1/2}+6p_{3/2})0_g^-$ levels.

L. Pruvost[1] and H. Jelassi[2]

[1] *Laboratoire Aimé Cotton, CNRS II, UPR3321, bat. 505, Campus d'Orsay, 91405 Orsay Cedex, France*

[2] *Centre National des Sciences et Technologies Nucléaires 2020 Sidi Thabet, Tunisie*

Abstract.

We report on the analysis of the $(6s_{1/2}+6p_{1/2})0_g^-$ weakly-bound levels of Cs_2 detected by photoassociation spectroscopy. We compare three methods of analysis: the use of the LeRoy-Bernstein formula, the use of the improved LeRoy-Bernstein formula and the use of the vibrational quantum defect. We show that the vibrational quantum defect method is more sensitive than the other methods and allows us to detect two deeply-bound levels of the $(6s_{1/2}+6p_{3/2})0_g^-$ potential, which are not detected by the others methods. The binding energies of the levels are found to be 565.49 cm^{-1} and 591.43 cm^{-1} below the $(6s_{1/2}+6p_{3/2})$ dissociation limit.

Keywords: Cold atoms, photoassociation, LeRoy-Bernstein formula, quantum defect.

PACS: 33.20.T, 32.80.Pj

1 Introduction

In the context of the formation of cold molecules prepared with cold atoms, many processes have been performed by photoassociation or magneto-association (Dulieu and Gabbanini, 2009). The photoassociation (PA) is the process which is most often applied. A conventional scheme to form cold molecules starts with the PA of a pair of cold atoms to a molecule, in an excited state. The next steps to form molecules in an electronic ground state are either the spontaneous decay of the excited molecule or the laser induced forced decay.

In any case, knowledge of the excited state is very important to understand the efficiency of the decay or to predict the best scheme to choose in order to form cold molecules.

Among the efficient schemes, some use an excited molecule whose wavefunction presents two regions of large probability. One of them is at large internuclear distance, which favors the photoassociation process from atoms (free state) to the excited state (bound state). The other region of probability is at short distance, which favors the Franck-Condon factor for decay of the excited state to a ground state. Such excited states exist as a combination of states of two different molecular potentials, one mainly at long range and the other at short range. The combination is produced via a coupling between the two molecular potentials. The coupling can be due to the spin-orbit interaction in the molecule or to the hyperfine interaction.

The spectroscopy of excited molecular levels provides data whose analysis allows one to detect coupling and therefore coupled states. In this context, PA spectroscopy (proposed in 1987, and demonstrated in 1993) is one of the most accurate methods, providing accurate values of energy levels and of rotational constants (Jones et al. 2006) (Stwalley and Wang 1999).

In this paper we compare three methods – the use of the LeRoy-Bernstein formula, the use of the improved LeRoy-Bernstein formula and the use of the vibrational quantum defect - for analyzing the data (energy levels) of Cs_2, obtained by Stwalley's group, concerning the 0_g^- levels lying close to the $(6s_{1/2}+6p_{1/2})$ dissociation limit (Pichler et al. 2004). We show that the method using the vibrational quantum defect is very sensitive and allows us to detect coupled states. With the available data, we have detected two regions with coupled levels. We have located the levels and determined the amplitude of the coupling and the wavefunction mixing. This paper completes data analyses presented in the two papers (Pichler et al. 2004, Pichler et al. 2006), where the authors used the original LeRoy-Bernstein formula or compared energy spacing with numerically calculated energies. With such methods, the authors did not detect coupled states, even if the calculation in Pichler 2006 indicates perturbations in energy regions when we observed the variations of the vibrational quantum defect.

The experimental data

The analysis that we present in this paper concerns experimental spectroscopic data for the $(6s_{1/2}+6p_{1/2})0_g^-$ state of Cs_2, obtained by Stwalley's group and reported in table II of reference

(Pichler et al. 2004). Stwalley's group reports on 31 levels detected below the dissociation limit. The binding energies of these weakly-bound levels range from 0 to 50 cm^{-1}.

The energy positions of the levels have been obtained by photoassociation spectroscopy of cold cesium atoms provided by a vapor-cell magneto-optical trap. In the PA process, a laser excites a pair of cold atoms and creates a molecule in an excited level of the Cs_2 molecule. This excited molecule decays very rapidly to a molecule in a level of the electronic ground state or to two hot atoms. In both decay processes, the products –a molecule or two hot atoms- are no longer trapped by the magneto-optical trap and, an atom loss is observed. The PA spectra are obtained by recording the atom loss (via the cloud fluorescence) while the laser wavelength is scanned. Due to selection rules in the PA process, three symmetries for molecular states are observed in the PA spectra starting from atoms in $6s_{1/2}$ state. Namely, 0_g^-, 0_u^+ and 1_g are observed. Due to the very low temperature of the atomic cloud, molecules are produced in levels with low J values (J=0 to 4). With the experimental resolution is 0.007 cm^{-1} the J lines are resolved and the binding energy of the J=0 level is thus well determined.

In this paper we consider the J=0 levels of the 0_g^- series, and we have not considered any rotational effect. In a previous paper we analyzed the data of the 0_u^+ symmetry (Jelassi et al. 2008). Here, with a similar approach, we focus on the 0_g^- one.

A pre-treatment of the experimental data is required to check if the levels are correctly identified. We checked the progression of the vibrational levels by plotting the energy difference between two consecutives levels versus the energy (figure 1). We plot on the same graph the energy spacing to the second neighbor as open dots. The plot of figure 1 is regular with a spacing increasing as a power law as a function of the energy except for regions with missing levels and for some other levels discussed below. Missing levels are detected because the spacing between two consecutive levels is placed on the second plot (spacing to the second neighbor). Some levels with binding energy @ 0.788 cm^{-1}, @1.786 cm^{-1}, @4.41 cm^{-1} and @ 38.740 cm^{-1} are not correctly consecutive in figure 1 . We think that these levels do not belong to the 0_g^- series but probably to another one. We have thus suppressed them and considered the new set of 27 data which are listed in table I. The attributed v values given in reference (Pichler 2004) have been corrected.

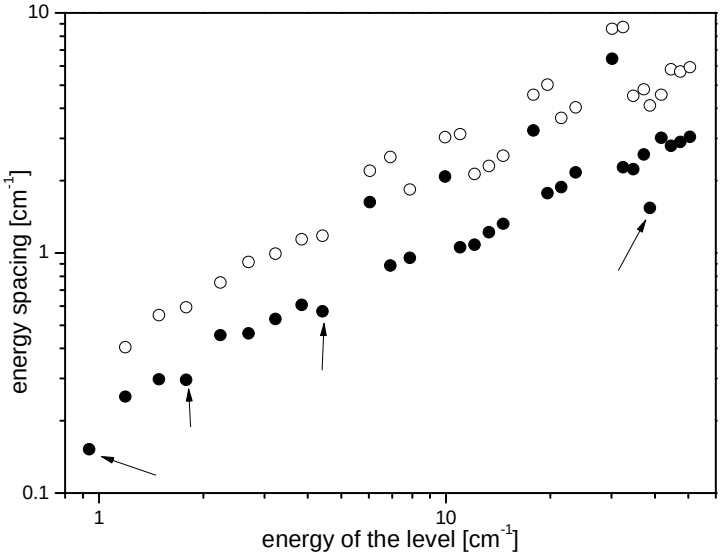

Figure 1: difference of the energy between two consecutive levels (dots) and to the second neighbor (opened dots) versus the energy. The arrows indicate the levels suspected to belong to another series.

Binding energy [cm^{-1}]	v	Binding energy [cm^{-1}]	v
0.94	11	14.63	29
1.192	12	17.865	31
1.49	13	19.638	32
2.241	15	21.517	33
2.704	16	23.682	34
3.234	17	30.118	37
3.842	18	32.395	38
6.037	21	34.629	39
6.923	22	37.199	40
7.875	23	41.756	42
9.95	25	44.551	43
11.006	26	47.453	44
12.086	27	50.498	45
13.305	28		

Table I: levels exacted from (Pichler et al. 2004) used in this study.

2 Analysis using the LeRoy-Bernstein formula and the improved LeRoy-Bernstein formula

2.1 The LeRoy-Bernstein formula.

In 1970, LeRoy, Bernstein and Stwalley established the energy law for levels of a potential varying as $-c_n/R^n$ (R>0) (LeRoy and R. B. Bernstein 1970; Stwalley 1970), The result relies on the use of the WKB (Wentzel – Kramers – Brillouin) method, and the Bohr-Sommerfeld quantization. First they have calculated the density of states. They have shown that in the energy region close to the dissociation limit, the density of states is given by an analytical expression which is a power law formula versus the binding energy. Then, in that case, the binding energy of each level is deduced from the density of states by integration over the energy variable. Because of the restriction of the WKB method, the result is only valid for weakly-bound levels. If ε denotes the binding energy of the level numbered by v, one gets by the so-called LeRoy-Bernstein (LRB) formula

$$v_D - v = \left(\varepsilon / E_n \right)^{(n-2)/2n} \qquad (1)$$

$$E_n = \left(\sqrt{\frac{\pi}{2\mu}} \frac{\hbar(n-2)}{c_n^{1/n}} \frac{\Gamma(1+1/n)}{\Gamma(1/2+1/n)} \right)^{2n/n-2} \qquad (2)$$

In formula (1), v_D is a constant, whose integer part gives the number of states and E_n is a factor given by formula (2) and depending on the c_n coefficient and the reduced mass μ. Γ indicates the gamma function.

The LRB formula has been extensively used to analyze molecular spectroscopy in energy ranges close to dissociation limits. The analyses were mainly fits of data plotting v versus the energy of the levels - using this formula and providing the value of E_n, thus values of c_n, for a given molecular series.

2.2 Expected value for E_6 of the 0_g^- state

For alkali-metal dimers, the asymptotic forms of the potentials are well-known because they are derived from the atomic dipole-dipole interaction. The form is $-c_3/R^3$ or $-c_6/R^6$ depending on the symmetry of the molecular state. In the Hund case (c), the 0_g^- potential curve, converging to $(6s_{1/2}+6p_{1/2})$ dissociation limit is asymptotically described by

$$V(R) = -c_6/R^6 \qquad (3)$$

Where R is the internuclear distance and c_6 a coefficient given by

$$c_6 = \frac{4C_3^2}{3A} + \frac{2C_6^{\Pi} + C_6^{\Sigma}}{3} \qquad (4)$$

In formula (4), A is an energy constant related to the fine structure of the cesium atom first p level by $3A/2=E(6p_{3/2})-E(6p_{1/2})$ and C_n coefficients are related to the atomic wavefunctions. For instance, C_3 is given by $C_3 = \langle 6s|r|6p\rangle^2 / 3$.

The value of A can be calculated using Steck data tables (Steck http://steck.us/alkalidata) and references therein: $A=1.68292\times10^{-3}$ a.u. The value of C_3 has already been discussed in reference (Jelassi et al. 2008), where we have compiled all the data available in the literature. Using 14 data we have concluded that $C_3=10.0391\pm0.0009$ a.u. The first part of c_6 is $4C_3^2/3A = 79847.9 \pm14.31$ a.u.

The values of C_6^{Π} and C_6^{Σ}, found in the literature are listed in the table II. With the values given in reference (Marinescu and Dalgarno 1995) (C_6^{Π}=11830 a.u., C_6^{Σ}=17390 a.u.) one obtains $(2C_6^{\Pi}+C_6^{\Sigma})/3$ =13683 a.u. As a consequence, the value of c_6 (the minimum one) is $c_6= 93.531\times10^3$ a.u. and the value of E_6 (the maximum one) is $E_6= 6.8966\times10^{-4}$ cm^{-1}.

Including the dispersion of the values observed in table II (except the 1984 and 1985 results), we would obtain $c_6= (9.3732\pm0.0229) \times10^5$ a.u and $E_6= (6.8825\pm0.0084)\times10^{-4}$ cm^{-1}.

C_6^{Π} (10^3 a.u.)	C_6^{Σ} (10^3 a.u.)	c6 (10^5 a.u.)	E_6 (10^{-4} cm^{-1})	reference
13.21	*19.81*	*9.5257*	*6.8338*	(Vigné–Maeder, 1984.)
18.61	*26.09*	*10.0951*	*6.6383*	(Bussery and Aubert-Frecon,. 1985)
11.83	17.39	9.3531	6.8966	(Marinescu and Dalgarno, 1995)
11.80	17.65	9.3598	6.8942	(Amiot et al. 2002)
11.76	18.2	9.3754	6.8884	(Amiot et al. 2002).
12.18	18.23	9.4045	6.8778	(Bouloufa, et al. 2007)
11.8925 ±0.1930	*17.8675 ±0.415*	*9.3732±0.0229*	*6.8825 ±0.0084*	Mean value (95-07)
13.2317±2.6912	*19.5617±3.3069*	*9.5189±0.2893*	*6.8382±0.1006*	Mean value (all)

Table II: values of C_6^{Π} and C_6^{Σ} found in the literature. Corresponding c_6 and E_6 values.

2.3 Application of LRB formula to Cs_2 0_g^- data

The data given in table I have been fitted using the LRB formula for n=6. In order to take into account an eventual energy shift, denoted ε_0, due to an eventual uncertainty about the dissociation limit, the fitting formula used was

$$v = v_0 + \left(\frac{\varepsilon-\varepsilon_0}{E_6}\right)^{1/3} \qquad (5)$$

The fitting procedure has been done in two cases, assuming either ε_0=0 or not. Results of the fits are given in table III. Even though the fit #2 has a better χ^2 value, the E_6 parameter is not in agreement with the expected value, given in the previous section, and differs by about 30 %. Such a discrepancy has already been observed for rubidium data (Jelassi et al. 2006a) and has been explained by an additional term in the LRB formula because of the incomplete 1970 LRB model. We also notice oscillations in the fit residual (see figure 2). The oscillations in the fit residual are also signatures of perturbation due to another series. In both figures 2 (a) and 2(b) (see next section) they occur in the vicinity of 11 cm^{-1} and 37 cm^{-1}. We will show in section 3 that the positions are those of perturbing levels

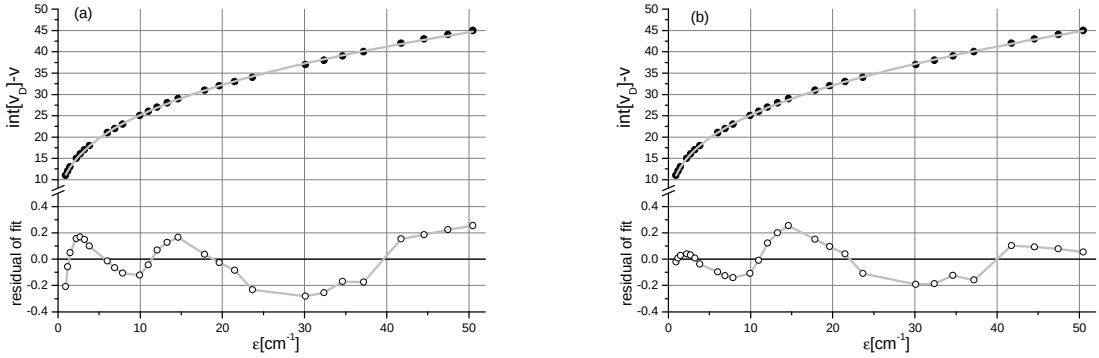

Figure 2: (a) data of table I versus the binding energy (dots) fitted by the LRB formula (grey line), and the residual of the fit (bottom cirve). (b) the same using the improved LRB formula.

	Fit #1	Fit #2	Fit #3
χ^2	0.0571	0.02729	0.01598
E_6 x10^{-4} cm^{-1}	5.179±0.069	4.723±0.095	6.5502±0.0488
v_0	-1.48±0.14	-2.89 ±0.29	-0.113 ±0.588
ε_0	0	0.368±0.076	0.0466±0.094
γ	0	0	0.04978±0.0109

Table III: results of the fitting procedures

2.4 Improved LRB formula.

The reexamination of the LRB formula has first been done by Comparat (Comparat 2004), and then by our group, in a slightly different way (Jelassi et al. 2006, Jelassi et al .2008b). Both works show that an additional term has to be added to the LRB formula in order to include short range effect of the potential. The first additional term is linear with the binding energy. The improved LRB formula is thus

$$v_D - v = \left(\frac{\varepsilon}{E_n}\right)^{(n-2)/2n} + \gamma\varepsilon \qquad (6)$$

where γ is the slope parameter which characterizes the correction due to the potential at small R values. The relation between γ and the short range potential is described in reference (Jelassi et al 2006a) and illustrated with some models.

The improved LRB formula has been successfully applied for alkali data, for instance 0_g^- and 0_u^+ symmetries (Jelassi et al. 2006a; Jelassi et al. 2006b; Jelassi et al 2007; Jelassi et al. 2008). This model also explains the slope in the plot of the vibrational quantum defect versus the energy.

We have used the improved LRB formula to analyze data of table I, and fitted them with the following formula

$$v = v_0 + \left(\frac{\varepsilon - \varepsilon_0}{E_6}\right)^{1/3} + \gamma(\varepsilon - \varepsilon_0)$$

As indicated in table III, the fit is better than in the case of original LRB formula. The χ^2 is reduced by a factor 2 compared to the previous fit. As shown in figure 2(b) the improved LRB formula allows us to reduce the residue of the fit for small and large binding energies. The value of E_6 delivered by the fitting procedure is close to the expected one. It differs only by 5% of the expected value calculated in section 3.2. Nevertheless, as it is shown in figure 2(b) the residue curve of the fitting procedure presents some oscillations. They are signatures of imperfections in the applied model.

3 Analysis using the vibrational quantum defect

3.1 Method

The imperfections of the LRB model can be analyzed by using the vibrational quantum defect approach. This approach, described in reference (Jelassi et al 2006a), is similar to the quantum defect theory previously used for Rydberg states of atoms and molecules.

The empiric use of the quantum defect approach consists first in converting the binding energy to an effective quantum number. For that, the levels are assumed to be described by a quantized energy law. In the case of Rydberg atoms, the law is the Rydberg one. In the case of vibrational long range levels, lying close to the dissociation limit, the law is the LRB one. In a second step, the effective quantum number is analyzed by its non integer part, which defines δ the quantum defect. The variation of δ is plotted versus the binding energy. The variation eventually shows the core effects or the presence of perturbing levels.

In our case, the energy levels are first converted to an effective vibrational quantum number by the relation

$$v^* = \left(\frac{\varepsilon}{E_6}\right)^{1/3}$$

which is the LRB law. Then the vibrational quantum defect is defined as the non-integer part of v* as

$$\delta = v^* - \mathrm{int}[v^*]$$

As soon as a set of data satisfied the LRB law, then the quantum defect is constant versus the energy and equal to int[v_D]. Otherwise, the variation of δ versus the energy shows the discrepancies relative to the given law, here the LRB law.

The application of the definition of v* requires a good knowledge of the binding energy, ε, and of the E_6 parameter. As shown in section 3.2, the value of E_6 is correctly known.

Knowledge of the binding energy requires a correct definition of the dissociation limit. As we have already discussed in section E of reference (Jelassi et al. 2008), the dissociation limit has to be defined relative to the ($6s_{1/2}$+$6p_{1/2}$) limit. Taking into account the hyperfine splitting is thus necessary to adjust the binding energy to the correct potential. To respect this limit we have shifted the values of table I by 0.168 cm^{-1}. This value is equal to $2\Delta_{hf1}+\Delta_{hf2}$, where $\Delta_{hf1}$is the hyperfine shift of $6s_{1/2}F=5$ and Δ_{hf2} is the hyperfine shift of $6p_{1/2}F'=4$.

The vibrational quantum defects extracted from table I (shifted by 0.168 cm^{-1}) are plotted versus the energy in figure 3. For this figure we have defined the quantum defect using the modulo 3, and not modulo 1, as it is defined in the formula. Such a definition is helpful to exhibit the variation of δ. The plot exhibits three plateaus separated by two regions with a strong variation in the vicinity of 11 cm^{-1} and 35 cm^{-1}. The plateaus are not exactly horizontal. Instead, the profile of the curve exhibits a linear increase, due to the linear term of the improved LRB formula.

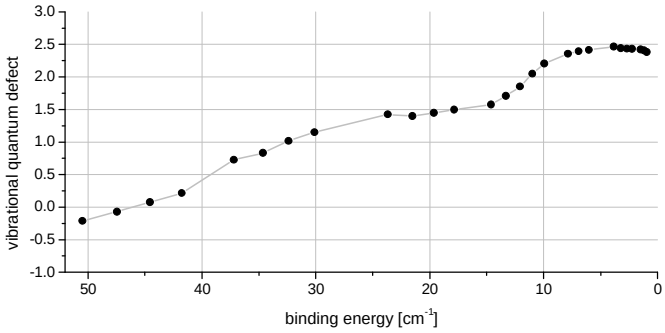

Figure 3: vibrational quantum defect versus the binding energy.

The rapid variations –steps- in such profiles are well-known in the physics of Rydberg states. They are the signatures of perturbing levels, belonging to another series which is coupled to the considered one. The steepness of the steps is connected to the coupling amplitude and to

the energy spacing of the coupled levels. Levels which are nearly resonant induce a steep step, even if the coupling is weak.

In the present case, we believe that we observe the perturbations of the $(6s_{1/2}+6p_{1/2})0_g^-$ levels due to levels (two levels) of the $(6s_{1/2}+6p_{3/2})0_g^-$ series, which is coupled to the $(6s_{1/2}+6p_{1/2})0_g^-$ levels due to the spin-orbit interaction.

A similar observation is reported at the end of section 4, in the reference (Pichler et al 2006) for calculated energy levels. The authors mention that the potentials are not coupled at long range distance and propose an explanation of the coupling due to interaction at the inner repulsive wall. They have not observed the coupling in the experimental data by using a conventional method. The explanation for the coupling is reasonable because in the studied energy region, we explore deeply bound levels of the $(6s_{1/2}+6p_{3/2})0_g^-$ potential.

Our approach does not permit to identify the origin of the coupling - namely long or short range- or if the molecular potential converging to the $(6s_{1/2}+5d_{3/2})$ limit plays an important role or not. Our approach allows us to determine an effective value of the coupling in the considered energy range (see the next section) and also the location of the perturbing levels.

3.2 Model to locate the perturbing levels

Figure 4 shows a usual plot of δ versus the energy. In that representation, which is close to a Lu-Fano graph, δ is defined modulo 1 and varies from 0 to 1. The steps observed in figure 3 appear as vertical lines in figure 4.

To interpret the observed profile, to determine the location of the perturbing levels and to characterize the coupling between the series, several models of two coupled series are usually applied. The simplest one assumes two series of regularly spaced levels, the energy spacing being denoted Δ_1 and Δ_2, which are coupled via a coupling assumed to be constant and denoted V (Demkov and Ostrovsky 1995). Even though this model is very simple, it is the root of others, which are more complicated, but start from a similar idea. A mathematical development of the model, which is given in reference (Jelassi et al. 2008) leads to an expression of the coupled system by a coupling equation,

$$\tan\left[\pi\frac{\varepsilon-E_1}{\Delta_1}\right]\times\tan\left[\pi\frac{\varepsilon-E_2}{\Delta_2}\right]=\pi^2\frac{V^2}{\Delta_1\Delta_2}$$

where ε is the energy, E_1 and E_2 are energies of unperturbed levels belonging respectively to the series 1 and 2. If V=0, the solutions are $\varepsilon=E_1+p\Delta_1$ and $\varepsilon=E_2+q\Delta_2$ (p and q being integers). For small values of V, the solutions for ε are close to these solutions, except when two levels (one of each series) are nearly resonant.

The coupling equation is easily adapted if the levels are not regularly spaced. The quantity $(\varepsilon-E_1)/\Delta_1$ is replaced by δ-μ, where δ is the quantum defect and μ the quantum defect at zero energy. In the situation where $\Delta_2 >> \Delta_1$ the coupling equation can be applied locally, i.e. over an interval $[E_2-\Delta_2,\ E_2+\Delta_2]$. Finally, the strength of the coupling is usually evaluated by

comparing V^2 and $\Delta_1\Delta_2$ (as in a two level problem) and is quantitatively given by a dimensionless parameter $K=V/(\Delta_1\Delta_2)^{1/2}$, with a strong coupling corresponding to K~1.

The coupling equation used to fit the plot of figure 3 is

$$\tan[\pi(\delta-\mu)]\times\tan\left[\pi\frac{\varepsilon-E_2}{\Delta_2}\right]=\pi^2K^2$$

In addition, the linear variation (see the improved LRB model) of the quantum defect is considered by adding $\mu=\mu_0-\gamma\varepsilon$. The fitting procedure, given by the grey line in the plot, provides the following values: μ_0=0.645±0.022; γ=0.01345±0.0012; E_2=11.45±0.28 cm^{-1}; Δ_2=25.94±0.58 cm^{-1}; K=0.1716±0.01.

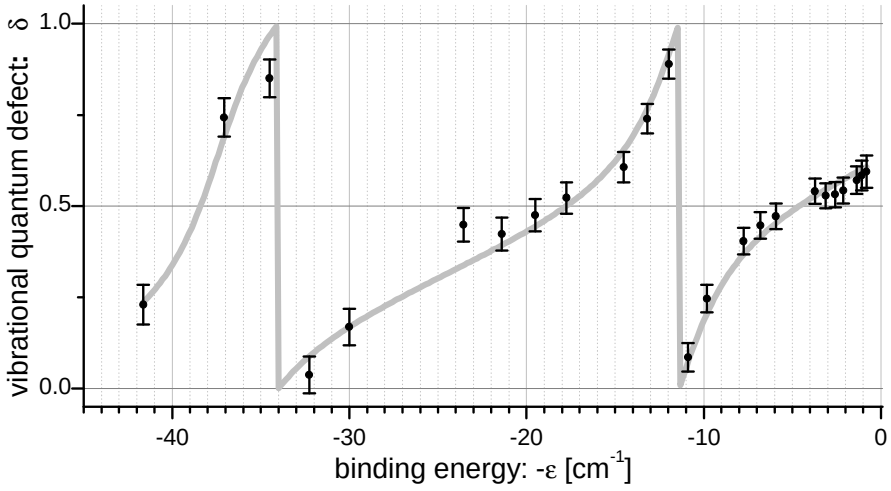

Figure 4: Vibrational quantum defect (dots) versus the energy, shifted by 0.12 cm^{-1} (note) Fitting curve (gray line) obtained with the parameters indicated in the text.

Such a model and procedure allow us to locate two levels of the $(6s_{1/2}+6p_{3/2})0_g^-$ series: @11.45 cm^{-1} and @37.39 cm^{-1} below the $(6s_{1/2}+6p_{1/2})$ dissociation limit. This result is in agreement with the observation done in the reference (Pichler et al. 2006).

Adding the fine structure of the cesium atom, the two levels are respectively @565.49 cm^{-1} and @591.43 cm^{-1} below the $(6s_{1/2}+6p_{3/2})0_g^-$ dissociation limit. We have found no experimental data concerning molecular levels of $(6s_{1/2}+6p_{3/2})0_g^-$ in this energy region. A calculation using the inner well of the potential curve would probably confirm our observation. Even if the positions of the two levels are not perfectly reproduced by the

calculation, it would be interesting to look at the spacing between them. We think that our observation could provide a way to adjust the depth of the $(6s_{1/2}+6p_{3/2})0_g^-$ potential.

3.3 Use of the fitting parameters to determine the wavefunction mixing.

The model provides fitting parameters which characterize the non-perturbed series. The series denoted 1 has levels whose energies satisfied the $(\varepsilon/E_6)^{1/3}=i+\mu_0-\gamma\varepsilon$ where i is an integer. Concerning the series denoted 2, the approach has given the location of two levels, namely $E_{2,1}=11.45$ cm^{-1} and $E_{2,2}=37.39$ cm^{-1}. The fitting procedure also provides the value of K, therefore the value of V.

A matrix representing the coupled systems can be built as

$$H=\begin{pmatrix} E_{2,1} & 0 & V & V & V & \dots \\ 0 & E_{2,2} & V & V & V & \dots \\ V & V & \varepsilon_1 & 0 & 0 & 0 \\ V & V & 0 & \varepsilon_2 & 0 & 0 \\ V & V & 0 & 0 & \varepsilon_3 & 0 \\ V & V & 0 & 0 & 0 & \dots \end{pmatrix}$$

Where ε_i are the solutions of $(\varepsilon_i/E_6)^{1/3}=i+\mu_0-\gamma\varepsilon$. Because of the small value of γ, we can use the approximation $\varepsilon_i\approx E_6(i+\mu_0-\gamma E_6(p+\mu_0)^3)^3$. The diagonalisation of H provides the wavefunction mixing.

In a crude approach, the wavefunction mixing were evaluated in a two level model, considering only one level of the series 1 and one level of the series 2. The matrix is then reduced to a 2x2 matrix ($H_{11}=E_{2,1}$; $H_{12}=H_{21}=V$; $H_{22}=\varepsilon_1$ for example). The eigenvalues are $(E_{2,1}+\varepsilon_1)/2\pm[(E_{2,1}-\varepsilon_1)^2+V^2]^{1/2}$ and the mixing is given by $\sin^2\theta$ where θ is defined by $\tan(2\theta)=2V/(E_{2,1}-\varepsilon_1)$.

In a more complete study, the wavefunction mixing were calculated in the frame of a multilevel model. We considered a more system composed by the two perturbing levels $E_{2,1}$ and $E_{2,2}$ and a set of levels $\{\varepsilon_i\}$. The values of ε_i were calculated by the improved LRB formula using fitting parameters. We have included 28 levels corresponding to i varying from 15 to 42 (energy range varying from 2.5 cm^{-1} to 51.5 cm^{-1}). Each couple $(E_{2,j}, \varepsilon_i)$ is coupled via a corresponding $V_i=K(\Delta_{1,i}\Delta_2)^{1/2}$ where Δ_2 is equal to the fit result and $\Delta_{1,i}$ varies with each level i using $\Delta_{1,i}=3E_6(i+\mu_0)^2$. Diagonalisation of the 30x30 matrix gives the eigenvalues and the corresponding eigenvectors. After diagonalisation, the new positions of the perturbing levels are found to be 11.843 cm^{-1} and 37.062 cm^{-1}. We deduce the wavefunction mixing for each level and the projection of the vector to the state $E_{2,1}$ or $E_{2,2}$ measures the $(6s_{1/2}+6p_{3/2})$ character of each level.

Both results – of the full diagonalisation and of the two-level approach- are given in figure 5. As expected, the multilevel model shows a more dilute coupling over a number of levels

larger than in the two-level-model. The $(6s_{1/2}+6p_{3/2})$ character of each level indicates that some levels would be adequate to be used in scheme of cold molecule formation. The spread of each shape in figure 5 shows that many levels of the $(6s_{1/2}+6p_{1/2})0_g^-$ series have a non negligible $(6s_{1/2}+6p_{3/2})$ character. Typically 10 levels dispatched over 10 cm^{-1} are involved. Such a configuration would be adequate for processes using a chirped laser (Luc-Koenig et al. 2004) to create cold molecules.

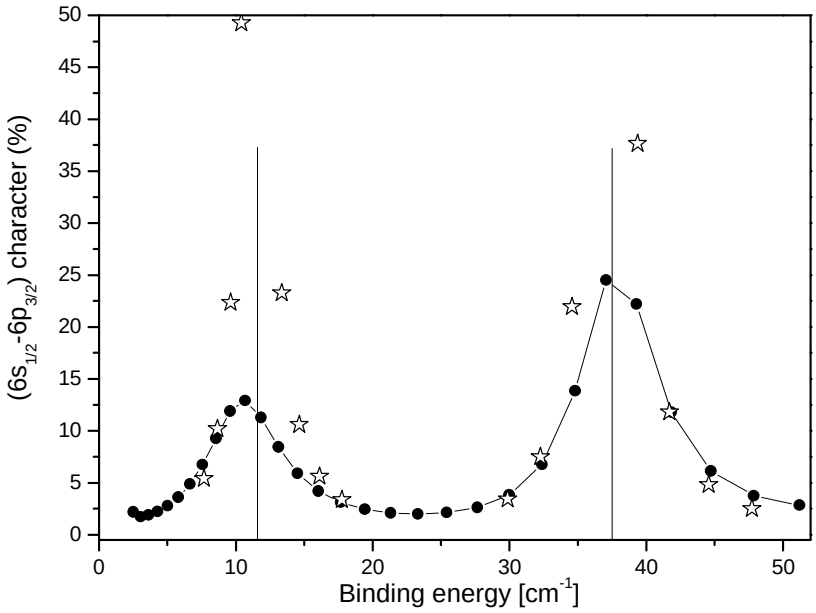

Figure 5: wavefunction mixing in a two-level approach (stars), and in the 30x30 matrix calculation (dots).Vertical lines (at $E_{2,1}$ and $E_{2,2}$) indicate the location of the perturbing levels being members of the $(6s_{1/2}+6p_{3/2})0_g^-$ series.

4 Conclusion

We have shown that we detect two levels of the $(6s_{1/2}+6p_{3/2})0_g^-$ series via their coupling to the $(6s_{1/2}+6p_{1/2})0_g^-$ levels lying close to the dissociation limit. Using the standard methods of LRB formula or improved LRB formula the coupling is not detectable. The method, which consists in extracting the vibrational quantum defect of the experimental data and to plot the variation versus the binding energy, is an accurate method to analyze precisely data and permit to exhibit coupling even though it is weak.

In the case of 0_g^- of Cs_2, studied here, we thus confirm observations in calculations presented in reference (Pichler et al. 2006). Furthermore, we locate the perturbing levels, evaluate the

coupling and deduce the wavefunction mixing. Such an approach is quite powerful to detect interesting mixing in the context of cold molecule physics.

Acknowledgements

We would like to thank Olivier Dulieu for stimulated discussions about this work, and Joshua Gurian for improving the manuscript.

The work is supported by IFRAF (Institut francilien de Recherche pour atoms Froids).

References

Amiot C, Dulieu O, Gutterres RF, and Masnou-Seeuws F 2002 Phys. Rev. A **66** 052506

Bouloufa N, Crubellier A and Dulieu O, 2007 Phys. Rev. A **75** 052501

Bussery B and Aubert-Frecon M 1985 J. Chem. Phys. **82** 3224

Demkov Y N, Ostrovsky V N 1995 J. Phys. B **28** 403

Comparat D 2004 J. Chem. Phys. **120** 1318

Dulieu O and Gabbanini C 2009 Rep. Prog. Phys. **72** 086401

Jelassi H, Viaris de Lesegno B, and Pruvost L 2006a Phys. Rev. A **73** 032501

Jelassi H, Viaris de Lesegno B, and Pruvost L 2006b Phys. Rev. A **74** 012510

Jelassi H, Viaris de Lesegno B, and Pruvost L 2007 AIP Conference Proceedings; FUNDAMENTAL AND APPLIED SPECTROSCOPY: Second International Spectroscopy Conference, ISC 2007 **935** 203

Jelassi H, Viaris de Lesegno B, Pruvost L, Pichler M, Stwalley W C 2008 Phys. Rev. A **78** 022503

Jelassi H, Viaris de Lesegno B, Pruvost L 2008b Phys. Rev. A **77** 062515

Jones K M, Tiesinga E, Lett P D, and Julienne P S 2006 Rev. Mod. Phys. **78** 483

LeRoy R J and Bernstein R B 1970 J. Chem. Phys. **52** 3869

Luc-Koenig E, Kosloff R, Masnou-Seeuws F, Vatasescu M. 2004 Phys. Rev. A **70** 033414

Marinescu M, Dalgarno A, 1995 Phys. Rev. A **52** 311

Pichler M, Chen H and Stwalley WC 2004 J. Chem. Phys. **121** 1796

Pichler M., Stwalley WC, Dulieu O, 2006 J. Phys. B: At. Mol. Opt. Phys. **39** S981-S992

Steck D , http://steck.us/alkalidata

Stwalley W C and Wang H 1999 Journal of Molecular Spectroscopy, **195** 194–228

Stwalley WC 1970 Chem. Phys. Lett. **6** 241

Vigné–Maeder F 1984 Chem. Phys. **85** 139

Note: Not 0.168 cm^{-1} as mentioned before: fitting procedures have been tested on data for energy shift varying from 0.1 to 0.2. Coupling values and location of the perturbing levels are not changed. The shift value of 0.12 cm-1 is coherent with variation of the vibrational quantum defect close to zero binding energy.